

# Volcanic Smoke Animation using CML

Ryoichi Mizuno<sup>†</sup>

<sup>†</sup>The University of Tokyo  
Tokyo, Japan

{mizuno,nis}@nis-lab.is.s.u-tokyo.ac.jp

Yoshinori Dobashi<sup>‡</sup>

<sup>‡</sup>Hokkaido University

Sapporo, Hokkaido, Japan

doba@nis-ei.eng.hokudai.ac.jp

Tomoyuki Nishita<sup>†</sup>

## Abstract

*The animation of volcanic smoke is useful for natural disaster simulations, entertainments, etc. In this paper, we propose a model to generate realistic animations of the volcanic smoke. The model is designed by taking the eruption magnitude decided by the eruption velocity and the initial volcanic smoke density, the buoyancy generated by the difference between the volcanic smoke density and the atmospheric density, and the decreasing of the volcanic smoke density due to the loss of the pyroclasts (fragments of magma); i.e., this model is based on the physical dynamics of the volcanic smoke. In this model, the Navier-Stokes equations are used, and we solve the equations by using the method of the Coupled Map Lattice (CML) that is an efficient solver. Hence, in our system, the behavior of the volcanic smoke can be calculated in practical calculation time, and various shapes of the volcanic smoke can be generated by only changing some parameters. Therefore, realistic volcanic smoke animations can be created by our approach efficiently.*

## 1 Introduction

Volcanic smoke animations could be used for natural disaster simulations, entertainments, such as movies, games. However, in the field of computer graphics, there is no method for simulating and visualizing the volcanic smoke based on physical laws. Although there are several commercial modeling products that can generate volcanic smoke animations [22], they can only obtain the motion of the volcanic smoke according to the orbits of some particles which are set by professional users. Therefore, the volcanic smoke animations generated by those products have less physical knowledge. Researchers in earth and planet science have proposed many models of

volcanic smoke behavior [9], but these models do cost a lot of time to solve some complex formulas to get highly strict results. In this paper, we propose an efficient model based on physical laws to generate realistic animations of the volcanic smoke in practical calculation time. There are many factors that decide the shape of the volcanic smoke. In these factors, the eruption magnitude, the buoyancy, the decreasing of the volcanic smoke density, and the temperatures of the magma and the volcanic smoke are important. Since the ascending current due to the temperature of the magma can be considered as the eruption velocity, and the buoyancy due to the temperature of the volcanic smoke can be considered as the buoyancy generated by the difference between the volcanic smoke density and the atmospheric density, the temperatures of the magma and the volcanic smoke can be simplified to enhance the simulation speed. Therefore, our model is designed by taking the following important factors that decide the shape of the volcanic smoke.

- Eruption magnitude:  
The eruption magnitude is decided by the eruption velocity and the initial volcanic smoke density, and it decides the scale of the volcanic smoke.
- Buoyancy:  
The buoyancy is generated by the difference between the volcanic smoke density and the atmospheric density. The conic shaped smoke that is a typical shape of the volcanic smoke is generated due to the buoyancy.
- Decreasing of the volcanic smoke density:  
The volcanic smoke density is decreased due to the loss of the pyroclasts. The diversities of the volcanic smoke shapes due to the differences of the contents inside the volcanic smoke are decided by the distribution varieties of the loss of the pyroclasts.

Moreover, we also present an efficient and stable solving method for our model by using the CML method [12], which is an efficient solver,

and the semi-Lagrangian advection scheme [14], which is a stable method even if the time step is large.

## 2 Related work

As described in the previous section, although there is no research for simulating and visualizing the volcanic smoke based on physical laws in computer graphics, but there are many researches for complex behavior of fluids such as smoke [4, 6, 14], cloud [1, 2, 10, 12], water [3, 5, 7], and flame [11, 13, 21]. Kajiya and Herzen proposed a simulation method for cloud by solving the Navier-Stokes equations [10]. However, at that time (1984), they could only calculate on very coarse grids due to the lack of the calculation ability of computer, and therefore their method could not generate realistic images. Foster and Metaxas proposed a method that can generate realistic motion of turbulent smoke on relatively coarse grids [6], but this method is stable only when the time step is very small and costs a lot of time for calculation. Stam introduced the semi-Lagrangian advection scheme to calculate the advection term of the Navier-Stokes equations stably even if the time step is large [14]. Moreover, Fedkiw *et al.* provided a technique called the vorticity confinement which is applied to Stam's model [4]. The vorticity confinement can represent small-scale vortices lost during the numerical calculation process. The methods provided by Stam and Fedkiw *et al.* premised for a small space such as inside a room or just a small area, so that their methods cannot take some factors, which are related to height, like the variation of the atmospheric density with height into consideration. Miyazaki *et al.* proposed a simulation method for cloud behavior by using the CML [12]. However, this method is specialized to generate the animations of the clouds, and cannot be applied to the volcanic smoke animation directly.

## 3 Model of volcanic smoke behavior

### 3.1 Atmospheric fluid evolution

The atmospheric fluid is incompressible and has small viscosity when its velocity is less than the sonic speed. Since the eruption velocity of the volcanic smoke is less than the sonic speed, the atmospheric fluid is assumed incompressible and as the non-viscosity fluid in our method. By this assumption, we can define the following incompressible and non-viscosity Navier-Stokes equations for the atmospheric fluid evolution.

$$\nabla \cdot \mathbf{u} = 0, \quad (1)$$

$$\frac{\partial \mathbf{u}}{\partial t} = -(\mathbf{u} \cdot \nabla) \mathbf{u} - \nabla p + \mathbf{f}, \quad (2)$$

where  $\mathbf{u} = (u, v, w)$  is a velocity vector of the atmospheric fluid,  $p$  is the pressure of the atmospheric fluid, and  $\mathbf{f}$  is an external force that is applied to the atmospheric fluid. Equation (1) means that the inflow and the outflow of a unit cell are balanced, and is called the "continuity equation". The first term of the right hand of Equation (2) means the advection of the atmospheric fluid along the velocity field, and is called the "advection term". The second term means the variation of the velocity caused by the gradient of the pressure, and is called the "pressure term". The third term means that the velocity is varied by the external force, and is called the "external force term".

In our method, we approximate Equation (1) and the pressure term of Equation (2) by using the method of CML (see [17, 18, 19, 20] for details). Therefore, we can obtain the following approximated Navier-Stokes equation.

$$\frac{\partial \mathbf{u}}{\partial t} = -(\mathbf{u} \cdot \nabla) \mathbf{u} + \eta \nabla (\nabla \cdot \mathbf{u}) + \mathbf{f}, \quad (3)$$

where  $\eta$  is a positive constant which means the rate of diffusion, and is called the "diffusion coefficient". The approximated Navier-Stokes equation does not need to be calculated iteratively to solve the continuity and the pressure effect, although iterative calculation is generally needed in other methods.

### 3.2 Volcanic smoke evolution

The volcanic smoke is transported by the atmospheric fluid, and the volcanic smoke density is decreased due to the loss of the pyroclasts. Therefore, we can define the following equation for volcanic smoke density  $\rho$ .

$$\frac{\partial \rho}{\partial t} = -(\mathbf{u} \cdot \nabla) \rho - \kappa(z) \rho, \quad (4)$$

where  $\kappa(z)$  is a function of height  $z$  and means the decreasing rate of  $\rho$ . In this paper, we call  $\kappa(z)$  as the "decreasing rate", and it should be set with the following two features.

- Near the crater, the volcanic smoke includes many large pyroclasts called the "volcanic blocks". Therefore,  $\rho$  decreases rapidly due to the fall of the volcanic blocks. To simulate this phenomenon, the decreasing rate needs to be set large in this region.
- In higher region, the volcanic smoke consists of many small pyroclasts called the "volcanic ash" and air, and then the pyroclasts are hardly lost. Therefore, the decreasing rate needs to be set small in this region.

The diversity of the volcanic smoke shapes due to the differences of the constituents of the volcanic smoke can be represented by setting the decreasing rate.

### 3.3 Buoyancy

Due to the difference between the volcanic smoke density and the atmospheric density, the buoyancy is occurred, which affects the velocity field of the atmospheric flow. Figure 1 shows the typical profiles of the densities of the volcanic smoke and the atmosphere. The buoyancy  $\mathbf{f}_{buoy}$  is defined as Equation (5). When the perpendicular component of  $\mathbf{f}_{buoy}$  is negative, the buoyancy works perpendicularly downward.

$$\mathbf{f}_{buoy} = \alpha(\rho_{atm}(z) - \rho)\mathbf{z}, \quad (5)$$

where  $\alpha$  is a positive constant which controls the strength of the buoyancy,  $\mathbf{z}$  is a perpendicularly upward unit vector  $(0,0,1)$ , and  $\rho_{atm}(z)$  is the atmospheric density, which is defined as an exponential function of height as the following equation.

$$\rho_{atm}(z) = \rho_0 \exp\left(-\frac{z}{H_e}\right), \quad (6)$$

where  $\rho_0$  is the atmospheric density at the ground ( $z=0$ ), and  $H_e$  is the degree of the atmospheric density variety with respect to height, and called the ‘‘scale height’’. The buoyancy plays an important role to decide the shape of the volcanic smoke, and the following dynamics generates the conic shaped smoke that is a typical shape of the volcanic smoke.

- In the region which height is low called the ‘‘gas thrust region’’, the atmospheric density is less than the volcanic smoke density (see Figure 1). Thus, the perpendicular component of  $\mathbf{f}_{buoy}$  becomes negative, and the buoyancy works perpendicularly downward. However, the momentum of the eruption is more dominant than the buoyancy. Therefore, the volcanic smoke is delivered toward upward.
- In the higher region called the ‘‘convective region’’, the atmospheric density is larger than the volcanic smoke density (see Figure 1). Thus, the perpendicular component of  $\mathbf{f}_{buoy}$  becomes positive, and the buoyancy works perpendicularly upward. Hence, the volcanic smoke is delivered toward upward.
- In the region higher than the convective region called the ‘‘umbrella region’’, the atmospheric density and the volcanic smoke density are almost balanced (see Figure 1). Therefore,  $\mathbf{f}_{buoy}$  becomes almost 0, and the volcanic smoke is not delivered perpendicularly no longer.

Our approach can generate realistic volcanic smoke images by satisfying these dynamics.

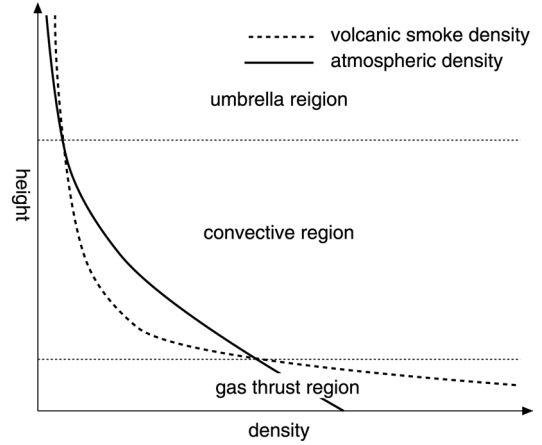


Figure 1: Typical profiles of the densities of the volcanic smoke and the atmosphere [16].

### 3.4 Representation of small-scale vortices

With the method which will be described in the next section, the volcanic smoke behavior can be calculated efficiently and stably, but some small-scale vortices may be lost due to the numerical calculation error. To solve this problem, we use a method introduced by Fedkiw *et al.* [4] to represent the small-scale vortices lost during the numerical calculation process by adding an external force  $\mathbf{f}_{conf}$  (see [15] for details). This method is called the ‘‘vorticity confinement’’, and  $\mathbf{f}_{conf}$  is defined by the following equations.

$$\mathbf{f}_{conf} = \varepsilon(\mathbf{N} \times \boldsymbol{\omega}), \quad (7)$$

$$\boldsymbol{\omega} = \nabla \times \mathbf{u}, \quad \mathbf{N} = \frac{\nabla |\boldsymbol{\omega}|}{|\nabla |\boldsymbol{\omega}||}, \quad (8)$$

where  $\varepsilon$  is a positive constant and means the degree of the vorticity confinement.

## 4 Efficient and stable solving method

In this section, the details of the solving method of our model are described.

### 4.1 Setting of simulation space

The simulation space is represented as  $n_x \times n_y \times n_z$  voxels. Each voxel is a cube with uniform size. The velocity vector  $\mathbf{u}$  and the volcanic smoke density  $\rho$  are defined as the state variables at the center of each voxel. As the initial state,  $\mathbf{u}$  is set to be a small value by using a random function, and  $\rho$  is set to be zero. But, for the voxels located to the mountain (the shaded

squares in Figure 2),  $\mathbf{u}$  is set to be a zero vector. Then, the decreasing rate  $\kappa(z)$  and the strength of the side wind  $\mathbf{f}_{wind}(z)$  at each height can be defined through a graphical user interface (GUI) shown in Figure 3, and the atmospheric density at each height  $\rho_{atm}(z)$  is defined by Equation (6).

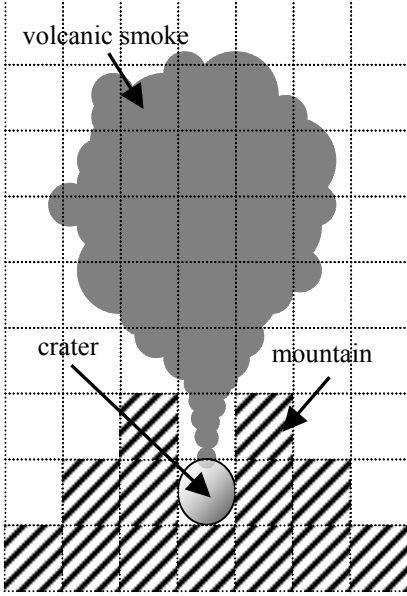


Figure 2: Outline of the simulation space.

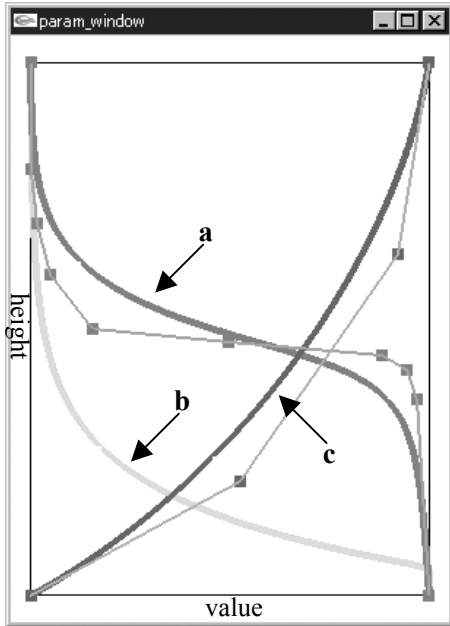


Figure 3: The GUI for setting the functions of height (a: decreasing rate, b: atmospheric density, c: strength of the side wind). The horizontal axis is the value of each function, and the vertical axis is height.

As shown in Figure 3, the decreasing rate and the strength of the side wind can be set by dragging the corresponding control points of the Bézier curves. Moreover, the atmospheric density

defined by Equation (6) is shown. Finally, the initial eruption velocity  $\mathbf{u}_{src}$  and the initial volcanic smoke density  $\rho_{src}$  that decide the eruption magnitude are assigned to the voxels correspond to the crater (the circle in Figure 2). It is also possible to make the volcanic smoke erupt with a spread. In our method, the diversity of the volcanic smoke shapes can be represented by only changing these parameters.

## 4.2 Sequential solving method

The time evolution of the volcanic smoke behavior can be obtained by iterating the following sequential processes: Add force  $\rightarrow$  Advect  $\rightarrow$  Project  $\rightarrow$  Decrease. “Add force” is the process to add the external force to the atmospheric fluid. “Advect” is the process to advect the state variables. “Project” is the process to vary the velocity with respect to the gradient of the pressure, and project the velocity vector to the divergent free field. “Decrease” is the process to decrease the volcanic smoke density with respect to the loss of the pyroclasts.

### 4.2.1 Add force

In Add force process, the effect of the external force as the third term of the right hand of Equation (3) is calculated. In our method, the external force  $\mathbf{f}$  is the sum of the buoyancy  $\mathbf{f}_{buoy}$ , the external force of the vorticity confinement  $\mathbf{f}_{conf}$ , and the strength of the side wind  $\mathbf{f}_{wind}(z)$ .  $\mathbf{f}_{buoy}$  is only applied to the voxels in which the volcanic smoke density  $\rho$  is larger than a threshold  $\rho_\epsilon (> 0)$ , so that the voxels are occupied by the volcanic smoke, hence  $\mathbf{f}_{buoy} = \mathbf{0}$  when  $\rho < \rho_\epsilon$ . By assuming that  $\mathbf{f}_{buoy}$  and  $\mathbf{f}_{conf}$  are unchangeable within a time step  $\Delta t$ , the equation for updating the velocity vector  $\mathbf{u}$  is expressed as follows.

$$\mathbf{u}^* = \mathbf{u} + (\mathbf{f}_{buoy} + \mathbf{f}_{conf} + \mathbf{f}_{wind}(z))\Delta t, \quad (9)$$

where  $\mathbf{u}^*$  is the velocity vector after being updated.

### 4.2.2 Advect

In Advect process, the effects of the advection as the first term of the right hand of Equation (3) and the first term of the right hand of Equation (4) are calculated. For this calculation, we use the semi-Lagrangian advection scheme. As illustrated in Figure 4, a path  $\mathbf{p}(\mathbf{x}, s)$  is defined as a parametric function of time parameter  $s$  by tracing a particle, which is located position  $\mathbf{x}$  to backward

along the velocity field at time  $t$ . Thus,  $\mathbf{p}(\mathbf{x}, s)$  represents a position that the particle existed at time  $(t-s)$ .

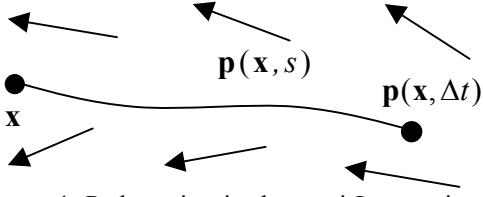


Figure 4: Path setting in the semi-Lagrangian advection scheme.

The state variables at position  $\mathbf{x}$  at time  $(t+\Delta t)$  are advected from position  $\mathbf{p}(\mathbf{x}, \Delta t)$ . Hence, the equations for updating the state variables are expressed as follows.

$$\mathbf{u}^*(\mathbf{x}) = \mathbf{u}(\mathbf{p}(\mathbf{x}, \Delta t)), \quad (10)$$

$$\rho^*(\mathbf{x}) = \rho(\mathbf{p}(\mathbf{x}, \Delta t)), \quad (11)$$

where  $\mathbf{u}^*$  is the velocity vector after being updated, and  $\rho^*$  is the volcanic smoke density after being updated.

#### 4.2.3 Project

In Project process, the effects of the pressure and the continuity as the second term of the right hand of Equation (3) are calculated. By using the CML method, a qualitative and efficient solution is achieved. The equation for updating the velocity vector  $\mathbf{u}$  is expressed as follows.

$$\mathbf{u}^* = \mathbf{u} + \eta \nabla (\nabla \cdot \mathbf{u}) \Delta t, \quad (12)$$

where  $\mathbf{u}^*$  is the velocity vector after being updated.

A discrete version of Equation (12) is shown in Equation (13). Here, we only describe the equation for updating  $u_{i,j,k}$ , which is the  $u$  component of the velocity vector  $\mathbf{u}(= (u, v, w))$  of voxel  $(i, j, k)$ .

$$\begin{aligned} u_{i,j,k}^* = & u_{i,j,k} + \eta [\{u_{i+1,j,k} + u_{i-1,j,k} - 2u_{i,j,k}\} / 2 \\ & + \{v_{i+1,j+1,k} - v_{i+1,j-1,k} - v_{i-1,j+1,k} \\ & + v_{i-1,j-1,k} + w_{i+1,j,k+1} - w_{i+1,j,k-1} \\ & - w_{i-1,j,k+1} + w_{i-1,j,k-1}\} / 4] \Delta t, \end{aligned} \quad (13)$$

where  $u_{i,j,k}^*$  is the  $u$  component of the velocity vector after being updated. The updating of the  $v$  and  $w$  components can be expressed in the same way.

#### 4.2.4 Decrease

In Decrease process, the decrease of the volcanic smoke density as the second term of the right hand of Equation (4) is calculated. The equation for updating the volcanic smoke density  $\rho$

is expressed as follows.

$$\rho^* = \rho - \kappa(z) \rho \Delta t, \quad (14)$$

where  $\rho^*$  is the volcanic smoke density after being updated.

## 5 Results

The images generated by our method are shown in Figures 5-9. Figures 5-8 show the volcanic smokes when there is no side wind. Figure 5 is the image to show the case when the decreasing rate in the gas thrust region is set to be relatively large, so that the volcanic smoke includes many large pyroclasts. Figure 6 shows the case when the decreasing rate in the gas thrust region is set to be relatively small, hence the volcanic smoke consists small pyroclasts and air. Figure 7 shows the case when the eruption velocity and the initial volcanic smoke density are relatively large, so that the eruption magnitude is relatively large. Figure 8 shows the case when the eruption velocity and the initial volcanic smoke density are relatively small, so that the eruption magnitude is relatively small. Besides the eruption velocity and the initial volcanic smoke density, the parameters in Figures 7 and 8 are set as those in Figure 5. Figure 9 shows a sequence of images of an animation of the volcanic smoke affected by the side wind. The parameters except the strength of the side wind are set as those in Figure 5.

Figure 10 shows photographs of real volcanic smokes for comparison. Figure 10a is a photograph of the conic shaped volcanic smoke, and Figure 10b is a photograph of the round shaped volcanic smoke. The shapes of smoke's outline in Figures 10a and 10b are similar to those in Figures 5 and 8, respectively.

Figure 11 shows the result of the simulation without the effect of the buoyancy. Besides the parameter of the buoyancy, other parameters are set as those in Figure 5. In this case, the volcanic smoke is not delivered to upward due to the lack of the buoyancy. Figure 12 shows the result of the simulation when the atmospheric density is constant. Besides the atmospheric density, other parameters are set as those in Figure 5. In this case, the upward buoyancy is dominant for voxels even in the umbrella region. Hence, the volcanic smoke is delivered to upward rapidly, so that the shape of the volcanic smoke is not conic but straight. Therefore, Figures 11 and 12 show that the buoyancy and the variety of the atmospheric density with height play important roles to generate the shape of the volcanic smoke.

All of the images are rendered as the simulation results with  $100 \times 100 \times 100$  voxels, by using the rendering software proposed by Dobashi *et al.* [2].

This rendering software can render the simulation result efficiently by utilizing graphics hardware. The computational time of the simulation was approximately 2.5 seconds per frame on a note PC (Pentium III 1.2GHz, 512MB RAM, GeForce3), and the computational time for the simulation almost depends on the number of voxels.

## 6 Conclusion and future work

In this paper, a method for creating realistic animations of the volcanic smoke is provided. The major features of our method are:

- The realistic behavior of the volcanic smoke based on physical laws is represented by considering the eruption magnitude decided by the eruption velocity and the initial volcanic smoke density, the buoyancy generated by the difference between the volcanic smoke density and the atmospheric density, and the decreasing of the volcanic smoke density due to the loss of the pyroclasts.
- Various shapes of the volcanic smoke can be generated on by only changing some parameters.
- An efficient and stable simulation is achieved by using the CML method and the semi-Lagrangian advection scheme.

To enhance the calculation speed of the simulation, it is a good idea to implement our model by using graphics hardware. Harris *et al.* proposed a fast calculation method of CML using graphics hardware [8] although graphics hardware is generally used for rendering. Implementation of the CML part of our model using graphics hardware will be a part of our future work.

## Acknowledgment

The authors would like to appreciate Prof. Nakada Setsuya, Mr. Ryo Miyazaki and Mr. Bing-Yu Chen for their supports to parts of this research.

## References

- [1] Y. Dobashi, K. Kaneda, H. Yamashita, T. Okita, and T. Nishita, A Simple, Efficient Method for Realistic Animation of Clouds, *Proc. SIGGRAPH 2000*, 31-37, 2000.
- [2] Y. Dobashi, T. Yamamoto, and T. Nishita, Efficient Rendering of Lightning Taking into Account Scattering Effects due to Clouds and Atmospheric Particles, *Proc. Pacific Graphics 2001*, 390-399, 2001.
- [3] D. P. Enright, S. Marschner, and R. Fedkiw, Animation and Rendering of Complex Water Surfaces, *Transaction on Graphics (Proc. SIGGRAPH 2002)*, 21(3): 736-744, 2002.
- [4] R. Fedkiw, J. Stam, and H. W. Jensen, Visual Simulation of Smoke, *Proc. SIGGRAPH 2001*, 15-22, 2001.
- [5] N. Foster and D. Metaxas, Realistic Animation of Liquids, *Graphical Models and Image Processing*, 58(5): 471-483, 1996.
- [6] N. Foster and D. Metaxas, Modeling the Motion of Hot, Turbulent Gas, *Proc. SIGGRAPH 97*, 181-188, 1997.
- [7] N. Foster and R. Fedkiw, Practical Animations of Liquids, *Proc. SIGGRAPH 2001*, 23-30, 2001.
- [8] M. J. Harris, G. Coombe, T. Scheuermann, and A. Lastra, Physically-Based Visual Simulation on Graphics Hardware, *Proc. SIGGRAPH / Eurographics Workshop on Graphics Hardware 2002*, 109-118, 2002.
- [9] Y. Ishimine and T. Koyaguchi, Numerical Study on Volcanic Eruptions, *Computational Fluid Dynamics Journal*, 8(1): 69-75, 1999
- [10] J. T. Kajiya and B. P. von Herzen, Ray Tracing Volume Densities, *Computer Graphics (Proc. SIGGRAPH 84)*, 18(3): 165-174, 1984.
- [11] A. Lamorlette and N. Foster, Structural Modeling of Natural Flames, *Transaction on Graphics (Proc. SIGGRAPH 2002)*, 21(3): 729-735, 2002.
- [12] R. Miyazaki, S. Yoshida, Y. Dobashi, and T. Nishita, A Method for Modeling Clouds based on Atmospheric Fluid Dynamics, *Proc. Pacific Graphics 2001*, 363-372, 2001.
- [13] D. Nguyen, R. Fedkiw, and H. W. Jensen, Physically Based Modeling and Animation of Fire, *Transaction on Graphics (Proc. SIGGRAPH 2002)*, 21(3): 721-728, 2002.
- [14] J. Stam, Stable Fluids, *Proc. SIGGRAPH 99*, 121-128, 1999.
- [15] J. Steinhoff and D. Underhill, Modification of the euler equations for "vorticity confinement": Application to the computation of interacting vortex rings, *Physics of Fluids*, 6(8): 2738-2744, 1994.

- [16] A. W. Woods, The fluid dynamics and thermodynamics of eruption columns, *Bull. Volcanol.*, 50: 169-193, 1988.
- [17] T. Yanagita, Coupled Map Lattice Model for Boiling, *Phys. Lett. A*, 165: 405-408, 1992.
- [18] T. Yanagita, Phenomenology for Boiling: A Coupled Map Lattice Model, *Chaos*, 3(2): 343, 1992.
- [19] T. Yanagita and K. Kaneko, Coupled Map Lattice Model for Convection, *Phys. Lett. A*, 175: 415-420, 1993.
- [20] T. Yanagita and K. Kaneko, Rayleigh-Bénard convection: Patterns, chaos, spatiotemporal chaos and turbulence, *Physica D*, 82: 288-313, 1995.
- [21] G. Yngve, J. O'Brien, and J. Hodgins, Animating Explosions, *Proc. SIGGRAPH 2000*, 29-36, 2000.
- [22] *Using MAYA: Dynamics (user's manual)*, 219-224, Alias|wavefront, 1999.

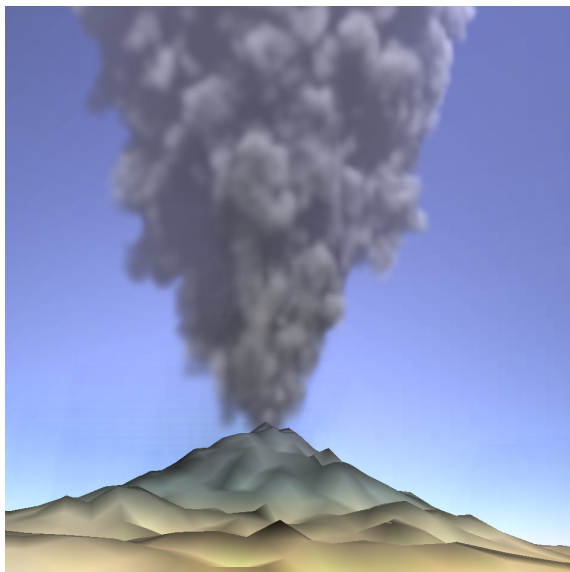


Figure 5: A conic volcanic smoke.

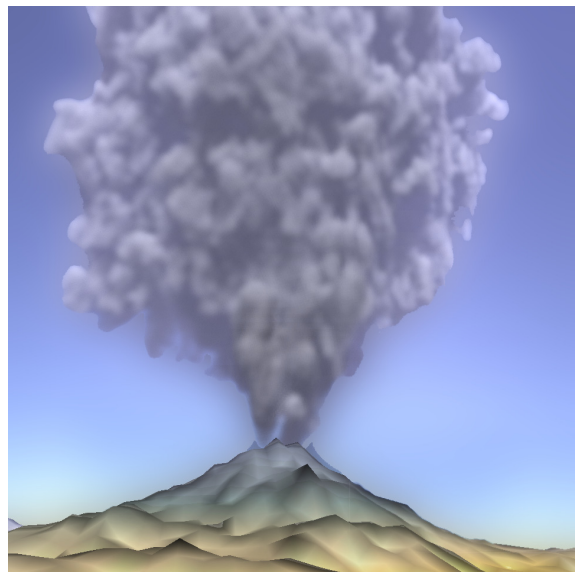


Figure 6: A spread volcanic smoke.

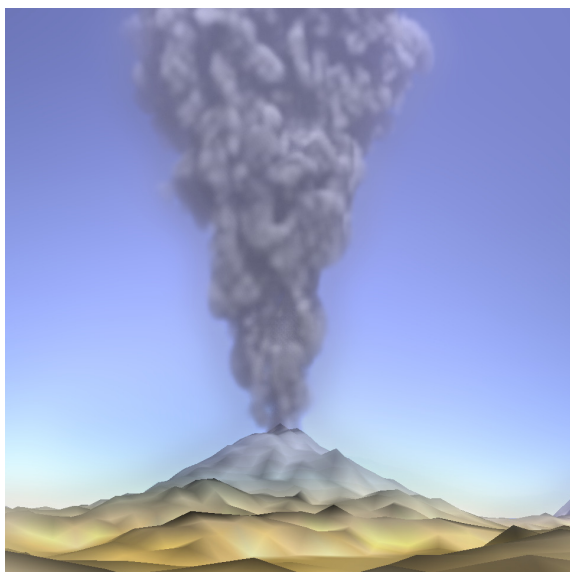


Figure 7: A volcanic smoke when the eruption magnitude is relatively large.

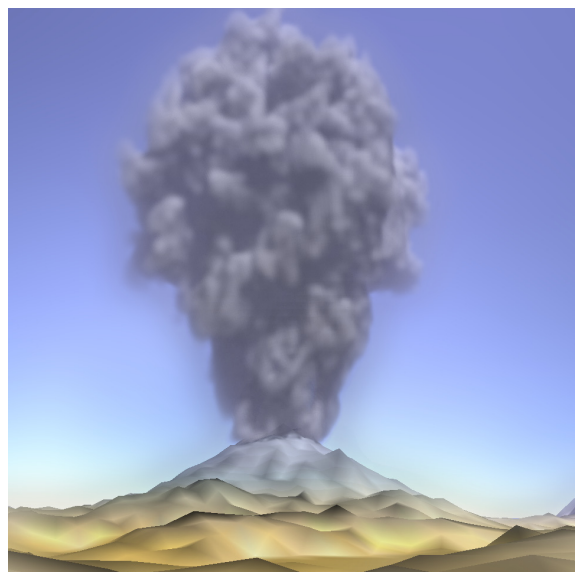


Figure 8: A volcanic smoke when the eruption magnitude is relatively small.

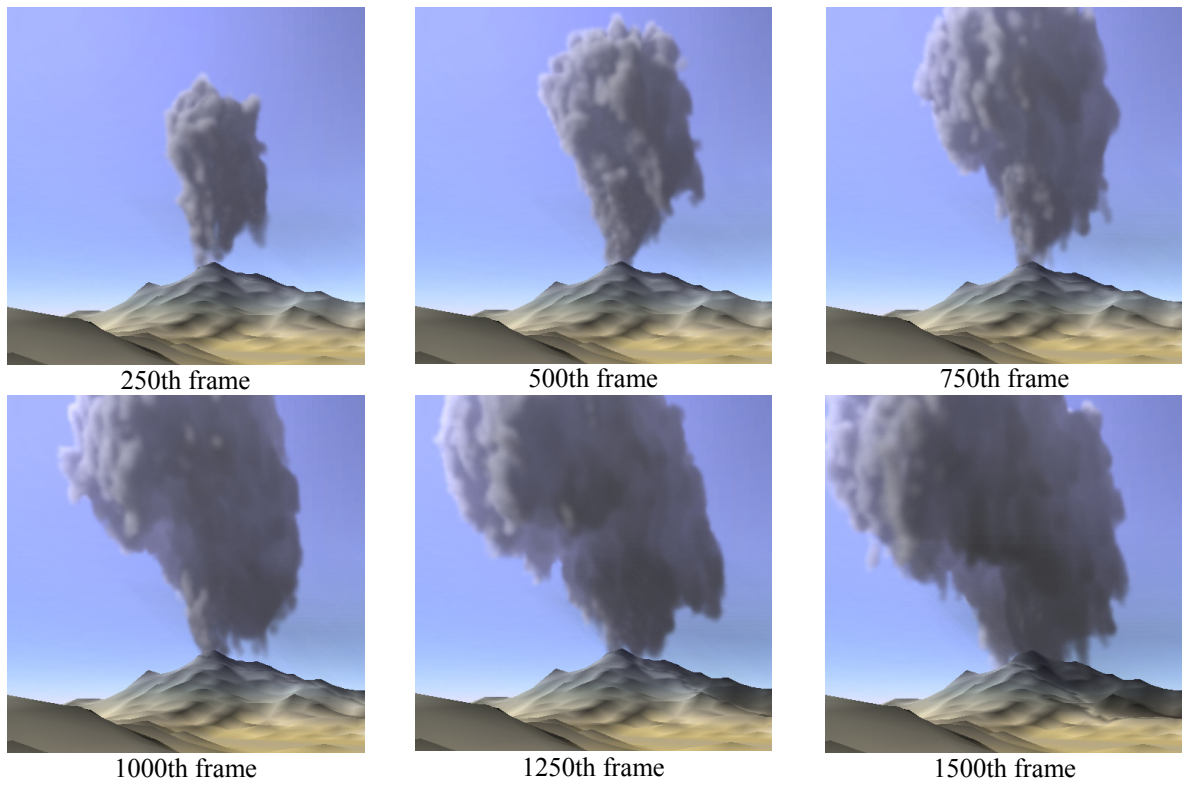


Figure 9: A volcanic smoke affected by the side wind.



a: similar to Figure 5

b: similar to Figure 8

Figure 10: Photographs of real volcanic smoke.



Figure 11: Result of the simulation without the buoyancy.



Figure 12: Result of the simulation when the atmospheric density is constant.